



Use microfluidics to create microdroplets for culturing and investigating algal cells in a high-throughput manner

Yu-Hsun Wang¹ · Yung-Shin Sun¹

Received: 13 September 2022 / Accepted: 24 March 2023 / Published online: 3 April 2023
© The Author(s), under exclusive licence to Springer-Verlag GmbH Germany, part of Springer Nature 2023

Abstract

Microalgae are essential sources of biofuels and bio-products, and usually they are studied using “bulk” technologies that ignore the heterogeneity of cells as well as the importance of single cell-based phenomena. As a consequence, being able to culture, monitor, and study single or a small amount of algal cells is important for investigating how the stochasticity of separate cells affects a population of them. Micro-droplets, micro-scaled aqueous droplets suspended in the oil phase, provide an excellent platform for investigating individual microalgae. They offer advantages of independence, small volume, mono-dispersion, high surface-area-to-volume ratio, and high throughput. In this study, a microfluidic device is designed and fabricated to generate micro-droplets for encapsulating microalgae of different culture media. The channel dimension and the flow rates of both aqueous and oil phases are adjusted based on simulation results to experimentally generate micro-droplets of similar sizes. This chip is then used to study how culture conditions, including various concentrations of nutrient solution, nitrogen (urea) and ion (Cu^{2+}), affect the growth of microalgae *Chlorella vulgaris* in a high-throughput manner. After 10 days of culturing and monitoring, the results show that, in general, the presence of nutrient solution and urea at optimal concentrations stimulates the growth of *Chlorella vulgaris*, while medium containing Cu^{2+} suppresses its growth. These findings can definitely help in optimizing the growth condition of microalgae for increasing their yields as resources of bio-products and biofuels.

Keywords Microalgae · Microdroplets · Microfluidic chip · High-throughput screening · Bioenergy

1 Introduction

Microalgae are unicellular species responsible for near half of the carbon fixation in the Earth’s atmosphere owing to their photosynthetic ability (Field et al. 1998). With sizes varying from few to a few hundred micrometers, microalgae can survive in either freshwater or marine systems, in either water column or sediment. Recently, microalgae are of much interest to researchers in both industry and academia because of their potential in yielding various bio-products, such as vitamins, pigments, fatty acids, and certain chemicals. Advantages of these microorganisms include high productivity, oxygenic photosynthesis, and no competition for arable land and water. (Parmar et al. 2011). For example, astaxanthin, a keto-carotenoid extracted from *Haematococcus*

pluvialis (*H. pluvialis*), is shown to prevent cardiovascular diseases, diabetes, and some neurodegenerative disorders. (Ambati et al. 2014; Panis and Carreon 2016). In addition, microalgae are good sources of ethanol and lipids for serving as biofuels, such as biodiesel, biobutanol, and biogasoline (Beer et al. 2009; Menetrez 2012; Radakovits et al. 2010; Singh and Singh 2014; Vo Hoang Nhat et al. 2018). The species as well as the growing conditions of these microalgae are known to affect their yields as bio-products and biofuels. Studies reveal that *H. pluvialis* produced astaxanthin in response to environmental stresses, such as light (excessive sunshine) and salt (increased salinity) (Lemoine and Schoefs 2010; Steinbrenner and Linden 2001), and certain species of algae produced lipids under nutrient limitation and mechanical stress (Mercer and Armenta 2011). Factors shown to affect the growth of microalgae include nutrient availability, pH value, temperature, salinity, inorganic carbon, oxygen, light intensity, and CO_2 (Khan et al. 2018). Therefore, to maximize the yields of algae-derived products, it is important to optimize their growth conditions.

✉ Yung-Shin Sun
089957@mail.fju.edu.tw

¹ Department of Physics, Fu-Jen Catholic University,
New Taipei City 24205, Taiwan

Conventionally, studies of microalgae are conducted using “bulk”-based methods where “average” effects are acquired (i.e., averaged over a large number of cells). For instance, light-dependent photosynthesis of *Chlorella vulgaris* (*C. vulgaris*) was investigated with a novel photosynthesis measurement system where all cells were approximated as the “average” cell (Yun and Park 2003). But in these “bulk”-based experiments, the heterogeneity of cells is not taken into consideration. As reported, genetically identical cells exposed to the same culturing conditions could exhibit significant variation in both molecular content and phenotypic characteristics (Kaern et al. 2005). As a result, it is of importance to culture and monitor single or a small amount of cells for investigating how the stochasticity of separate cells affects a population of them.

With advantages of mono-dispersion, independence, small volume, high surface-area-to-volume ratio, and high throughput, micro-droplets provide an excellent platform for single cell-based studies (Hayat and El Abed 2018; Zhu and Wang 2016). Single or multiple cells cultured inside droplets are considered as in three-dimensional (3D) in vitro micro-environments (Jang et al. 2016). In the example of single cell analysis, the dispersed fluids (containing single cells) can be antibody-contained culture medium for screening of specific antibody-secreted cells (Mazutis et al. 2013), lysis buffer for DNA-sequencing (Eastburn et al. 2014), or drug-contained culture medium for screening drug library (Brouzes et al. 2009). Single cells encapsulated within these partitions may secrete biomolecules that are easily detected, facilitating the rapid detection of target cells by fluorescence-activated cell sorting (FACS) (Wu et al. 2013). A variety of microorganisms have been investigated in micro-droplet-based systems, including yeast (Beneyton et al. 2017), bacteria (Jakiela et al. 2013), and even *Caenorhabditis elegans* (*C. elegans*) (Stegeman et al. 2019).

Microfluidic devices having micro-fabricated structures integrated with fluidic components possess advantages of small volume, low cost, and easy fabrication. Especially in cell-related studies, only a small amount of cells and reagents is consumed compared with traditional cell culture dishes and microplates (El-Ali et al. 2006; Nan et al. 2014). Because in vivo tissue cells are subject to various fluidic stresses including blood and all kinds of body fluids, these in vitro devices provide a platform best mimicking the fluid-circulating micro-environment. Moreover, within these minimized chips, different chemical and physical stimuli can be applied to cells in a precise and controllable manner to investigate their responses. For example, collective cell migration, such as chemotaxis, electrotaxis, and phototaxis, has been extensively investigated in microfluidic devices (Li and Lin 2011; Lin et al. 2019; Sun 2017). When applying microfluidics in generating microdroplets, micro-scaled aqueous droplets are suspended in an oil stream within a micro-scaled

channel. In a microfluidic device, droplets can be generated either passively or actively (Zhu and Wang 2016). Passively, flow-focusing, co-flow, or cross-flow generators are applied to introduce the dispersed fluid (such as water) into the continuous fluid (such as oil) by squeezing, dripping, jetting, tip-streaming, and tip-multi-breaking modes (Farjami and Madadlou 2017; Zhu and Wang 2016). In these cases, the channel dimension and the flow rates of both aqueous and oil phases play important roles in determining the droplet size and the generation rate. Micro-droplets can be manipulated for various purposes such as serving as reservoirs for incubation, being separated to allow different operations on identical duplicates for increasing experimental throughput, being injected with a variety of chemicals and gene materials by pico-injection and on-chip droplet sorting and detection by combining lasers and electrodes (Best 2016).

However, in almost all studies, micro-droplets generated in microfluidic devices are monodispersed, meaning that the medium condition within each droplet is identical. This highly limits the experimental throughput in screening against different culture media and investigating how they affect the growth of microalgae. In this study, a microfluidic device is designed and fabricated for generating microalgae-encapsulated micro-droplets with various concentrations of nutrient solution, nitrogen (urea), and ion (Cu^{2+}). Microalgae incubated within these compartments are monitored for 10 days to track their numbers over time, and the results indicate that, in general, the presence of nutrient solution and urea at optimal concentrations stimulates the growth of *Chlorella vulgaris*, while medium containing Cu^{2+} suppresses its growth. These findings are helpful in optimizing the growth of microalgae as bio-resources, and this platform can be further applied to single cell-based investigations of more complicated animal and human cells in a high-throughput way.

2 Materials and methods

2.1 Chip design and fabrication

The fabrication and the observation of micro-droplets were conducted in two separate chips, namely the fabrication chip and the observation chip, respectively. The designs were drawn in AutoCAD (Autodesk, USA) for making masks, and the devices were fabricated using the standard soft-lithography technique. In brief, after a negative mode of SU-8 GM1070 (EM RESIST LTD., UK) was fabricated on a 4-inch silicon wafer, PDMS (Dow Corning, USA) and a curing agent in a ratio of 10:1 were used to replicate the mold to form the microstructures. Via O_2 -plasma activation at 18 W for 40 s under an O_2 pressure of 600 mTorr (Harrick Plasma, USA), the PDMS layer was bonded onto a

glass slide to form the integrated chip. Figure 1a shows the design and picture of the fabrication chip. The height and the width (except the inlets, the outlets, and the nozzles where two phases meet) of the microfluidic channels are 55 and 200 μm , respectively. The size of the nozzles is 60 μm . The dispersed phase (the upper part in the 2D schematic) mimics the “Christmas tree” geometry beginning with two inlets, with one having the max concentration (for example, 1) and the other having the minimum one (for example, 0). After the first separation and mixture, concentrations of 1, 0.5, and 0 can be achieved. Finally, concentrations of 1, 0.875, 0.5, 0.125, and 0 can be attained after the third separation and mixture in the five downstream outlets (shown in blue in the 3D schematic). Here, it is assumed that all liquids split-flow smoothly and equally around the fork. By this means, micro-droplets containing five different concentrations of

medium can be generated. The design and the picture of the observation chip are shown in Fig. 1b. The height of the channels is 55 μm , and micro-pillars with a size of about 400 $\mu\text{m} \times 1000 \mu\text{m}$ are created inside the chambers to prevent them from collapse.

2.2 Simulation of flow rates and concentrations

The commercial software COMSOL Multiphysics (COMSOL, Inc., USA) was used for numerical simulation of flow rates and concentrations inside the dispersed-phase channels of the microfluidic chip. The “Laminar Flow” and “Transport of Dilute Species” modules were applied with the following parameters and settings: the boundary condition for inlets is “velocity”: normal inflow velocity; the boundary condition for outlets is “pressure”: 101,300 Pa with normal flow and

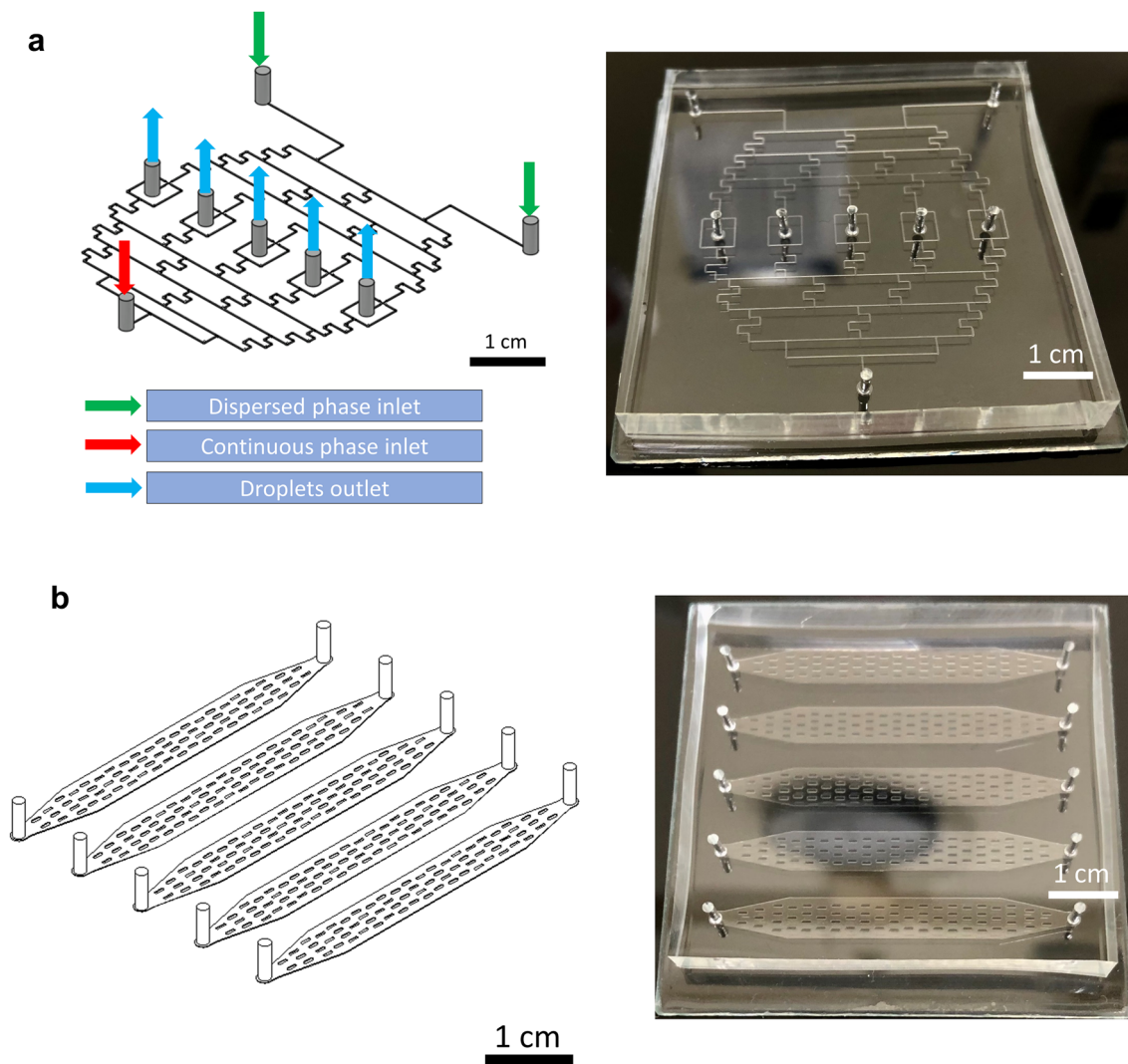


Fig. 1 a 3D schematic (left) and picture (right) of the droplet-fabrication microfluidic chip. b 3D schematic (left) and picture of the droplet-observation microfluidic chip

suppress backflow; diffusion coefficient = 2.8×10^{-9} m²/s for Brilliant Blue FCF (used for testing the distribution of concentrations); inlet flow rate = 100 μ L/min (set in each inlet); concentrations = 0 and 100% in two inlets, respectively.

2.3 Algae preparation and chemicals

Green microalgae *Chlorella vulgaris* (*C. vulgaris*) were used as the model for investigating the effects of medium conditions on their growth. As a freshwater specie, these unicellular green algae are spherical in shape, about 2 to 10 μ m in diameter, and are without flagella. They are widely used as food supplement for their good antioxidant and therapeutic properties. Before seeding into the microfluidic chip, these microalgae were cultured in the 1 \times medium under the exposure of a white LED light source (VITALUX X1, Taiwan) at room temperature without extra CO₂ supply. The light intensity was about 29 μ mol photons m⁻² s⁻¹ and the rhythm was 16/8 (16-h light and 8-h dark). 1 \times medium contains 1 mL of F/2 nutrient solution diluted in 1 L of 10/1000 sterilized sea water. F/2 nutrient solution is composed of 1: 1: 1 of NaNO₃ (75 g/L), NaHPO₄ (5 g/L), and FeCl₂·6H₂O (6.3 g/L) + Ethylene-diamine-tetra-acetic acid (EDTA) (8.72 g/L). 0 \times medium contains sea water only. CuSO₄·H₂O is dissolved in 1 \times medium to get desired Cu²⁺ concentrations. The urea solution is prepared by diluting it in 1 \times medium to attain the desired concentration.

2.4 Experimental system and procedure

As shown in Fig. 1a, the flow-focusing geometry is used to generate micro-droplets. First, the nozzles were filled with the continuous-phase liquid. Then the dispersed-phase liquid approached the junction, forming the immiscible interface. Finally, by continuously flowing in both liquids, the interface was broken and uniform droplets were formed. The continuous-phase inlet (see Fig. 1a in red) was connected to a syringe containing a mixture (Fluigent, France) (*w/w*) of 98% 3 MTM NovecTM 7500 fluorinated oil and 2% dSURF, a high-performance surfactant used in forming the water–oil interface of the micro-droplet. The two dispersed-phase inlets (see Fig. 1a in green) were connected to two syringes containing suspensions of *C. vulgaris* microalgae at desired culturing mediums. Algae concentration was adjusted so that there were about 0–4 cells in each droplet, and the average encapsulate ratio was about 50% (50% of the droplets contained no cells). Various concentrations of nutrient solution, nitrogen (in urea), and Cu²⁺ (in CuSO₄·H₂O) were prepared to investigate their effects on the growth of microalgae. For example, as two dispersed liquids having Cu⁺² concentrations of 0 and 5 μ M, concentrations of 0, 0.625, 2.5, 4.375, and 5 μ M could be attained within micro-droplets in five outlets. All syringes were connected to syringe pumps (New

Era, USA) with flow rates of 400 and 100 μ L/min set in the continuous and dispersed inlets, respectively. After flowing in all liquids for few minutes, stable micro-droplets were generated and then, for long-term storage, transferred into five separate glass culture tubes (Kimble, Germany, diameter = 5 cm) via Teflon tubes (VICI Jour, Switzerland, diameter = 0.5 mm). The culture tube was sealed with a PDMS-made plug to prevent from evaporation. The tube was filled with FC-40 (3 M, USA), a surfactant for maintaining the integrity of micro-droplets. During the whole period of culturing, the tubes were exposed to a white LED light source under the same condition as described in Sect. 2.3. To count the numbers of algae within micro-droplets, each culturing tube was connected to one channel of the observation chip. With a peristaltic pump (HONDWEN, Taiwan), droplets were sucked into the channel. The chip was mounted on top of an inverted microscope (ESPA SYSTEMS Co., Taiwan) for taking bright-field images under a magnification of 100 \times . Afterward, microalgae-encapsulated droplets were pushed back into the culturing tubes again using the peristaltic pump. These steps were repeated daily for taking time-dependent images.

2.5 Data analysis

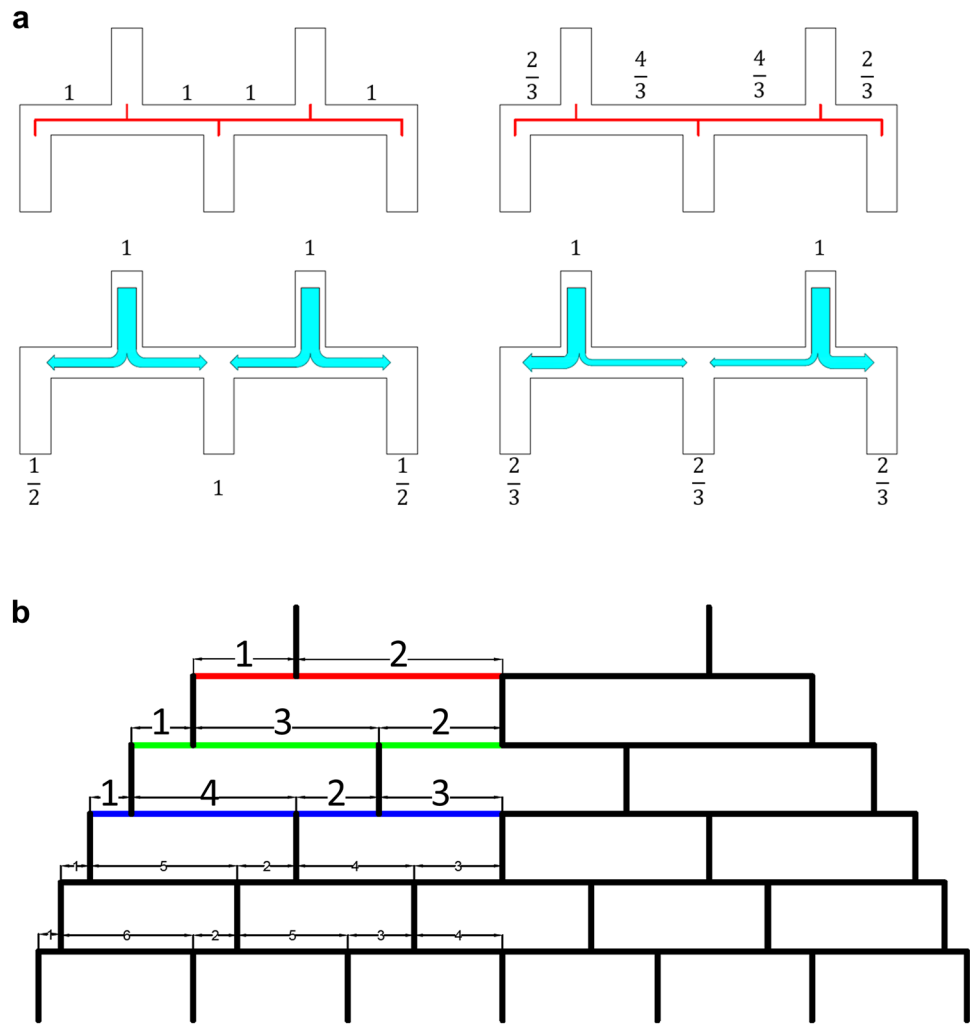
For quantifying the sizes of generated microdroplets, images of five droplets-contained channels in the observation chip were taken. For each channel, at least 10 droplets were selected, and their sizes were measured using the ImageJ software (National Institute of Health, USA). The mean values together with the standard deviations (SDs) were calculated. The growth of microalgae under different culture conditions was tracked by taking images of five channels of the observation chip in a one-day time interval. For each channel at one time-point, at least two pictures were taken, with each containing at most 40 micro-droplets. For statistical analysis, the numbers of algae within at least 20 droplets from two independent experiments were counted manually to get the mean and SD (as the error bar) for a specific medium condition at one certain time. Droplets were selected randomly with each containing at least one cell.

3 Results and discussion

3.1 Simulation of flow rates and concentrations

The “Christmas tree” structure is commonly used for creating concentration gradients for cell-related experiments, such as chemotaxis and electrotaxis (Lo et al. 2013; Wu et al. 2015). In a traditional design of equal separations (1:1:1:1 in Fig. 2a, left), the flow rates are different in all outlets (Jeon et al. 2000). Since these rates play an

Fig. 2 Theoretical evaluation of how the geometry of the chip affects the flow rates in all outlets. **a** Left: the unmodified design (top) with flow rates of 1:2:1 in three outlets (bottom). Right: the modified design (top) with flow rates of 1:1:1 in three outlets (bottom). **b** The design can be further extended to, for example, a six-layered device



crucial role in determining the size of micro-droplets (Kim et al. 2012; Wojnicki et al. 2018), the geometry of the microfluidic chip has to be modified to make these values almost the same in all outlets. The inequality in flow rates can be well explained by the Hagen–Poiseuille equation, equivalent to the Ohm’s law in electric circuits. To calculate the theoretical flow rates in all outlets, the law of conservation of mass is applied at each node. Given that the flow rate is affected by the resistance of the channel, and this resistance is directly proportional to the channel length, the easiest way to modify the geometry to attain the same flow rates in all outlets is to adjust the ratio of split-channel lengths. After a series of calculations, Fig. 2a right shows the optimal two-layered structure where the flow rates are equal in all three outlets. And as shown in Fig. 2b, this design can be further extended to infinitely many layers. The present modified microfluidic chip is supposedly capable of attaining similar flow rates in all outlets and therefore generating microdroplets of similar sizes. Unless otherwise specified, the modified design is

used in the microfluidic device for both dispersed and continuous phases.

The COMSOL numerical simulations of flow rates inside the dispersed-phase channels (see Fig. 1a left in green) of both unmodified and modified microfluidic chips are indicated in Fig. 3a. Figure 3b shows the flow rates plotted along the red line (the locations of nozzles) at a depth of 30 μm. For the unmodified structure, a Gaussian distribution in the flow rates was clearly observed, with a mean of 0.2124 m/s and a SD of 0.0176 m/s. In this design, these unequal flow rates of the dispersed phases might cause non-uniform droplet sizes. After modification, the flow rates were almost the same in all five outlets, being 0.2038 m/s in average with a SD of only 0.00084 m/s. Based on these results, we also modified the design of the continuous-phase channels (see Fig. 1a left in red) so that the ratios of the flow rates of the dispersed phase to those of the continuous phase in all nozzles were nearly equal.

This microfluidic device is designed to generate microdroplets containing five different concentrations of medium.

Fig. 3 **a** Numerical simulations of flow rates inside the dispersed-phase channels for unmodified (right) and modified (left) microfluidic chips. **b** Flow rates plotted along the red line in **a** at a depth of 30 μm . Such modification significantly reduces the differences in flow rates among all outlets

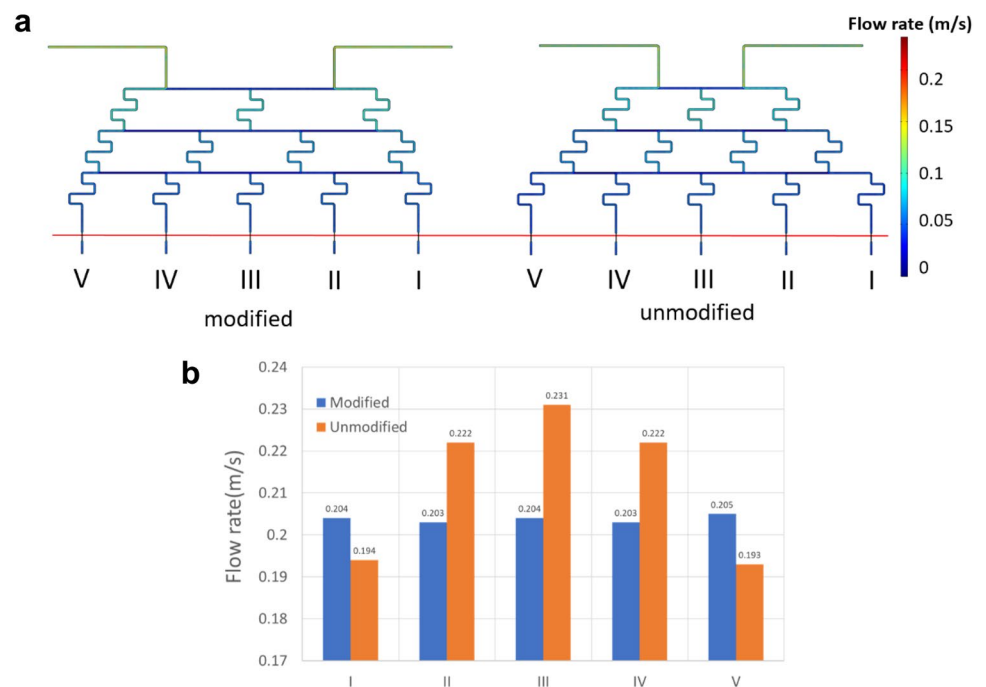


Figure 4a shows the COMSOL numerical simulations of blue dye concentrations inside the dispersed-phase channels of both unmodified and modified microfluidic chips. The concentrations in the left and right inlets are 100 (in dark red) and 0% (in dark blue), respectively. Again, Fig. 4b shows the flow rates plotted along the red line at a depth of 30 μm . As clearly indicated in the figure, the concentrations were not significantly affected by the modification. For the modified design, the simulated concentrations in the first (I), second (II), third (III), fourth (IV), and fifth (V) outlets were about 0, 21, 50, 78, and 100%, respectively. Although some

of these values are not close to the theoretical ones (0, 12.5, 50, 87.5, and 100% from I to V), the modified design with stable and precise concentrations can be used in fabricating microdroplets of different contents.

3.2 Characterization of micro-droplet sizes and concentrations

Figure 5a shows the images of micro-droplets within five channels of the observation chip. Their sizes in radii were characterized using the ImageJ software, as indicated in

Fig. 4 **a** Numerical simulations of blue dye concentrations inside the dispersed-phase channels for unmodified (right) and modified (left) microfluidic chips. **b** Concentrations plotted along the red line in **a** at a depth of 30 μm

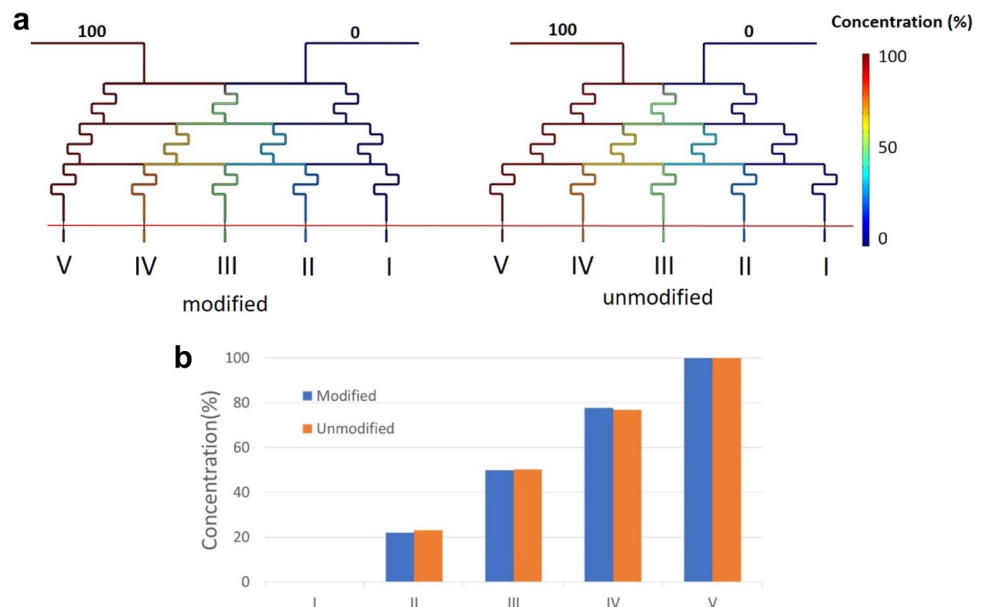


Fig. 5 **a** Images showing micro-droplets in five channels of the observation chip. **b** Average sizes (in radii) of microdroplets in these channels

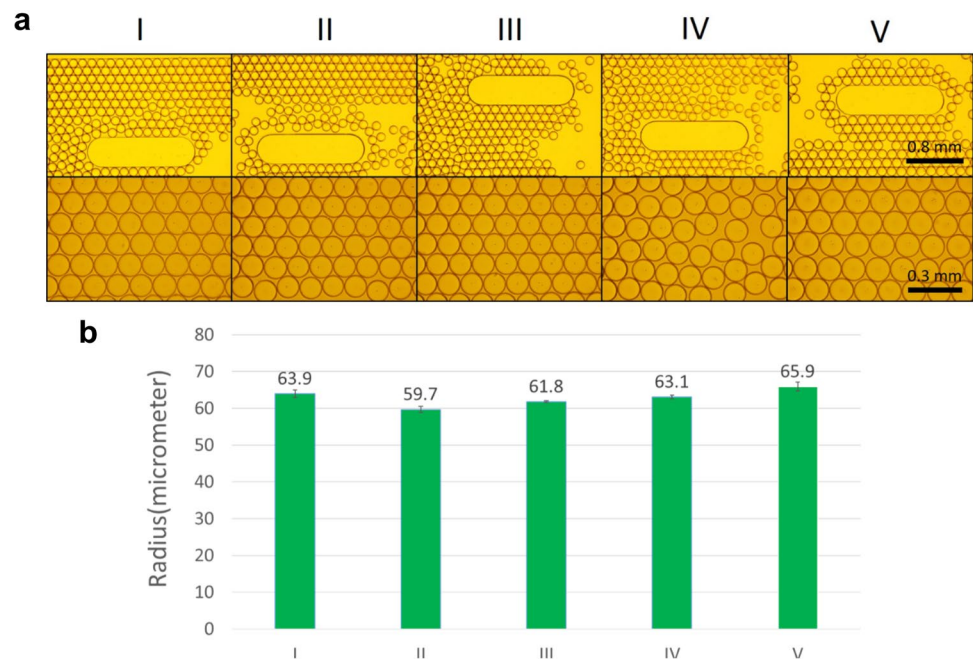


Fig. 5b. These micro-droplets exhibited high mono-dispersity both in individual channels and across five channels. The mean radii with SDs in channel I, II, III, IV, and V were 63.9 ± 0.97 , 59.68 ± 0.88 , 61.8 ± 0.21 , 63.06 ± 0.55 , and 65.88 ± 1.2 μm , respectively. Across all channels, the average radius was 62.87 μm with a SD of 2.32 μm . This corresponds to a droplet volume of around 1.04 nL. With flow rates of 400 and 100 $\mu\text{L}/\text{min}$ set in the continuous and dispersed inlets, respectively, the flow rate ratio (FRR) is calculated to be simply 2. The FRR is defined as the ratio of the flow rate of the side channel (the continuous phase) to that of the center channel (the dispersed phase). By controlling the geometry (the nozzle size) as well as the flow rates in two immiscible phases, the micro-droplet size can be well regulated. Gulati et al. reported microfluidic droplet formation in flow-focusing geometries possessing varying degrees of rounding (Gulati et al. 2016). A variety of junction geometries differing in their radii of curvature (R) and corners of rounding (either symmetric or asymmetric) were fabricated. The largest droplets were produced at the junctions with the largest rounding of asymmetric $R = 50$ μm (Gulati et al. 2016). It was also found that the diameter of micro-droplets (in the asymmetric $R = 50$ μm case) decreased from around 225 to 100 μm with increasing FRR from 1 to 8 (Gulati et al. 2016). A similar trend was observed in a microfluidic T-junction where the mean droplet volume decreased from about 6.5 to 2.5 nL with an increase in the FRR from 0.4 to 2 (Loizou 2018).

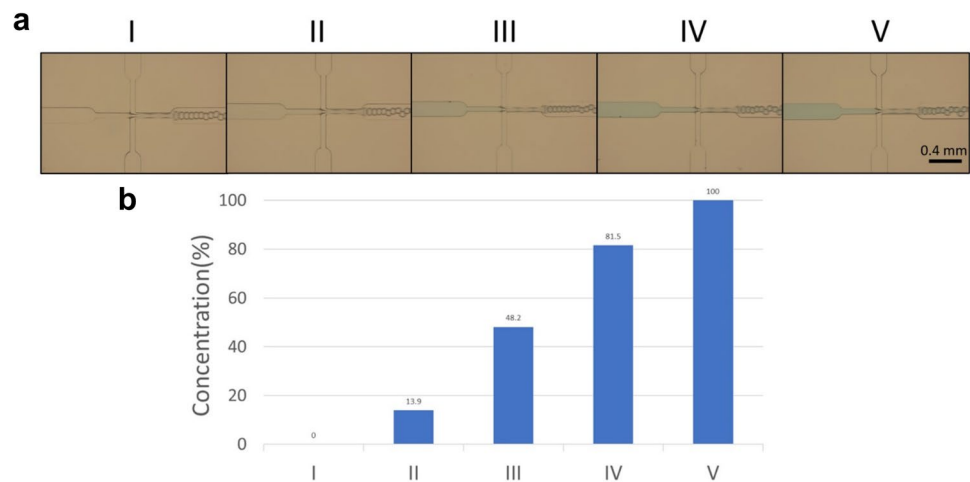
As mentioned earlier, one of the main advantages of the present chip is that it can generate microdroplets of five different culturing conditions. Five sets of droplets are

synthesized simultaneously, greatly increasing the experimental throughput. To experimentally verify the distribution of concentrations, blue dye (0.05% (w/v) bromophenol blue) in deionized (DI) water and DI water only were continuously flowed into the two inlets of the dispersed phase. A much cheaper oil (98% Paraffin oil + 2% surfactant Span 80, both from Sigma, USA) was used as the continuous phase. Then the whole chip was imaged using an inverted microscope. Figure 6a shows the images of micro-droplets, in five channels of the fabrication chip, right next to the nozzles. As indicated, the blue colors were getting darker and darker from channel I to V. In Fig. 6b, the intensities were quantified by measuring the gray values with ImageJ and then normalized, showing that concentrations of 0 , 13.9 , 48.2 , 81.5 , and 100% were attained in five channels. These values are comparable to those in simulations, suggesting the applicability of this chip in parallel analysis of algae growth under different media. Microfluidic devices with a similar design were used to study the effects of antioxidant concentrations on the production of reactive oxygen species (ROS) in lung cancer cells (Lo et al. 2013), investigate the effects of ultraviolet lights on human fibroblasts (Huang et al. 2017), and evaluate the correlation between cell migration and ROS under electric field stimulation (Wu et al. 2015).

3.3 Effects of culture media on the growth of *Chlorella vulgaris* algae

The evaporation of microdroplets was investigated by monitoring their sizes over time. After 10 days of observation, droplets with $1 \times$ medium showed no significant shrinkage.

Fig. 6 Using blue dye as the sample, the concentrations within micro-droplets are quantified. **a** Images showing microdroplets right next to the nozzles. **b** Quantified, normalized concentrations by measuring gray values of the microdroplets in (a)



Also, due to the presence of the surfactant FC-40, coalescence was not observed.

3.3.1 Culturing *Chlorella vulgaris* in microdroplets

Figure 7a shows the images of *C. vulgaris*-encapsulated droplets with 1× medium at a series of time points up to 10 days. Qualitatively, these green algae grew in a time-dependent manner. The numbers of cells per droplet in each of the five channels were counted each day and illustrated in Fig. 7b. In general, microalgae growth is characterized in five phases including lag, exponential, declining growth rate, and stationary and death phases (Rahman et al. 2020). Usually, optimal harvesting of algae biomass is performed at the exponential or stationary phases as these are the two with the highest cell biomass (Rahman et al. 2020). It was reported that an exponential growth is expected if algal cells are not limited by external factors such as nutrient or light supply (Golterman et al. 1975). In the exponential phase, the growth curve can be fitted to

the equation: $N_2 - N_1 = e^{(t_2 - t_1)\mu}$, where N_2 and N_1 are the numbers of algae at time t_2 and t_1 , respectively, and μ is the growth rate (Liang et al. 2013). As shown in the figure, except some irregularities in channel I at some time points, algae grew with almost the same rates in all five channels. The numbers of algae per droplet increased from < 2 at day 0 to around 15 at day 10. By fitting these data to the exponential equation, the growth rates were 0.256, 0.267, 0.284, 0.251, and 0.27 d^{-1} in channel I, II, III, IV, and V, respectively. This resulted in a mean value of 0.265 d^{-1} and a SD of 0.0117 d^{-1} , indicating a very slight variation in growth rates among all channels. The growth rate highly depends on the culture conditions, such as components of the medium, pH value of the medium, environmental temperature, light exposure, and cell density (Bialon and Rath 2018; Nguyen et al. 2019). Wong et al. conducted a growth medium screening for *C. vulgaris* growth. Among 13 different media, maximum and minimum growth rates of 0.278 and 0.042 d^{-1} were found for the Bold basal and Fog

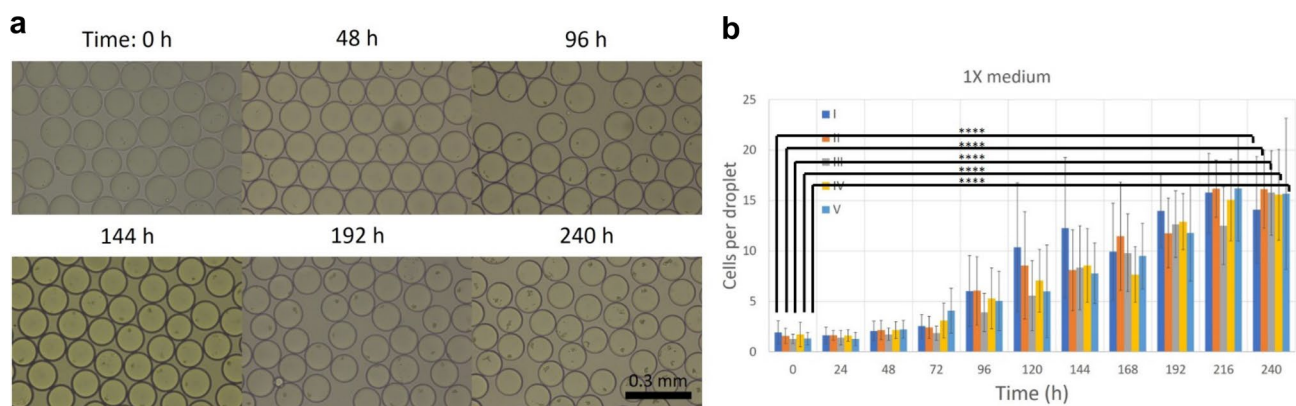


Fig. 7 **a** Images showing algae-encapsulated micro-droplets with 1× medium at different time points. **b** Quantitative data showing the growth of *C. vulgaris* when cultured in different channels, all with

1× medium. Statistical analysis was performed. ns: no statistically significant difference ($p > 0.05$); * $p < 0.05$; ** $p < 0.01$; *** $p < 0.001$; **** $p < 0.0001$

media, respectively (Wong 2017). A similar study reported *C. vulgaris* growth rates of 0.34 and 0.1 d⁻¹ for the BG-11 and F/2 media, respectively (Khemiri et al. 2022).

3.3.2 Effects of F/2 nutrient solution on the growth of *Chlorella vulgaris*

To study the effects of F/2 nutrient solution on the growth of *C. vulgaris*, 0× (containing no F/2) and 2× media (containing 2 mL/L F/2) were flowed into the two inlets of the dispersed-phase channels. This resulted in five different nutrient concentrations in five sets of microalgae-encapsulated microdroplets. The algae growth was monitored for 10 days, with four representative images shown in Fig. 8a. As qualitatively seen in the figure, algae grew faster in the presence of 2× medium. Quantitatively, for each medium concentration, the numbers of algae per droplet were counted at a time interval of 1 day. As shown in Fig. 8b, *C. vulgaris* didn't grow without the or with just a little supply of F/2 nutrient solution. The numbers of cells per droplet remained below 2 under 0× and 0.25× media. As the concentration increased beyond 1×, algae grew noticeably. For example, the numbers increased from <2 at day 0 to around 11 at day 10 under 1× and 1.75× media. Unexpectedly, under a concentration of 2×, cells didn't grow as well compared to those in 1× and 1.75×. In terms of growth rates, the fitted values were 0.05, 0.073, 0.254, 0.268, and 0.209 d⁻¹ for 0×, 0.25×, 1×, 1.75×, and 2× media, respectively. From these results, it is suggested that a highly nutrient medium could cause adverse effect to the growth of *C. vulgaris*. The effects of culture medium contents on the growth and lipid production of *C. vulgaris* have been widely investigated (Crofcheck 2012; Khemiri et al. 2022). It was found that the KNO₃-based medium worked the best for *C. vulgaris*, while additional media components, such as EDTA and vitamin

B, didn't result in a significant increase in algae growth. (Crofcheck 2012) Khalili et al. investigated the effects of various nutrients concentrations in the growth medium on the biomass production of *C. vulgaris* (Khalili et al. 2015). Similar to the findings in the present study, the growth rate was not always proportional to the nutrient concentration. For example, the optimal concentrations of MgSO₄·7H₂O and K₂HPO₄ in the growth medium were 0.06 (instead of 0.1) and 0.04 (instead of 0.1) g/L, respectively (Khalili et al. 2015). To the best of our knowledge, this study is the first one to reveal the dependence of F/2 nutrient concentration of the growth of *C. vulgaris*.

3.3.3 Effects of urea on the growth of *Chlorella vulgaris*

Urea, the most frequently applied nitrogen fertilizer in agriculture, is shown to trigger algal blooms in adjacent water bodies (Huang et al. 2014). To evaluate how urea affects the growth of *C. vulgaris*, 0 and 2 mL/L of urea were flowed into the two inlets of the dispersed-phase channels to attain concentrations of 0, 0.25, 1, 1.75, and 2 mL/L in five sets of algae-encapsulated droplets. Figure 9a shows the images of these microdroplets with 0 and 2 mL/L of urea at day 0 and day 10. It is obvious that *C. vulgaris* grew significantly in both conditions, but the number of cells per droplet was larger in the 2 mL/L case. Quantitative data are shown in Fig. 9b, indicating that the algae grew over time under any of the urea concentrations. However, urea concentrations of 1 and 1.75 mL/L seemed to stimulate the growth the most. The numbers of algae per droplet increased from <2 at day 0 to around 51 and 59 at day 10 for urea concentrations of 1 and 1.75 mL/L, respectively. Again, increasing the concentration of urea didn't further accelerate the growth. The number was about 43 at day 10 for 2 mL/L of urea. These observations were also verified by fitted growth rates of

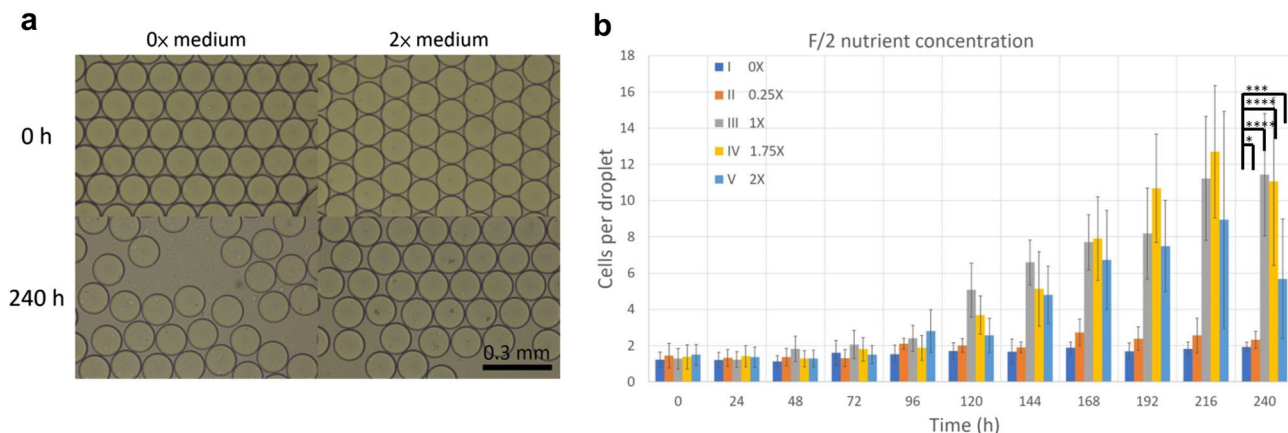


Fig. 8 a Images showing algae-encapsulated micro-droplets with 0× and 2× media at 0 h and 240 h. **b** Quantitative data showing the growth of *C. vulgaris* when cultured in different concentrations of

F/2 solution. Statistical analysis was performed. ns: no statistically significant difference ($p > 0.05$); * $p < 0.05$; ** $p < 0.01$; *** $p < 0.001$; **** $p < 0.0001$

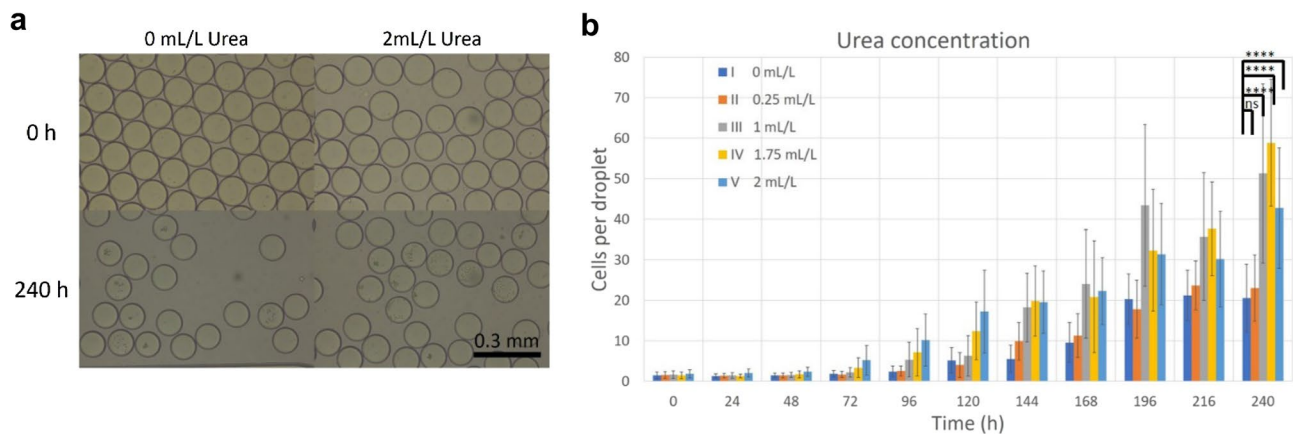


Fig. 9 **a** Images showing algae-encapsulated micro-droplets with 0 and 2 mL/L of urea in culture media at 0 h and 240 h. **b** Quantitative data showing the growth of *C. vulgaris* when cultured in differ-

ent concentrations of urea. Statistical analysis was performed. ns: not statistically significant difference ($p > 0.05$); * $p < 0.05$; ** $p < 0.01$; *** $p < 0.001$; **** $p < 0.0001$

0.325, 0.336, 0.413, 0.408, and 0.3409 d^{-1} for urea concentrations of 0, 0.25, 1, 1.75, and 2 mL/L, respectively. Similar findings were observed in other studies but with different optimal concentrations and culture media. Fiebiger et al. observed that there was generally a positive relationship between urea concentration and *C. vulgaris* growth, but the growth decreased after the limit (Fiebiger 2018). The average amounts of cell growth were 1.88×10^5 , 5.94×10^5 , 8.12×10^5 , and 1.57×10^5 cells/mL per week for urea concentrations of 0, 0.1, 0.2, and 0.3 mL/L in water (Fiebiger 2018). Among a variety of nitrogen sources for *C. vulgaris* growth including sodium nitrate (NaNO_3), urea ($\text{CO}(\text{NH}_2)_2$), ammonium chloride (NH_4Cl), and ammonium carbonate ($(\text{NH}_4)_2\text{CO}_3$), urea was found to be the optimal one (Khalili et al. 2015). And after 7 days of examination, the optimal level of urea in BG-11 medium was about 0.19 mL/L, leading to a maximum biomass concentration of 1.23 g/L (Khalili et al. 2015). In contrast, urea concentrations of 0.1 and 0.76 mL/L gave biomass concentrations of 1.1 and only 0.6 g/L, respectively (Khalili et al. 2015). It has been shown that urea could be toxic at high concentrations (Converti et al. 2006), which might inhibit algae growth.

3.3.4 Effects of $[\text{Cu}^{2+}]$ on the growth of *Chlorella vulgaris*

Heavy metals including copper (Cu), chromium (Cr), zinc (Zn), cadmium (Cd), and lead (Pb) were reported to affect algae in suppressed cell division, inhibited growth rate, restrained enzyme activity, and reduced photosynthesis (Ouyang et al. 2012). It was found that treatments of Cu, Cr, Zn, Cd, and Pb at critical concentrations significantly inhibited the growth of *C. vulgaris*, while Cu/Cr had an inhibiting effect and Zn/Cd had a promoting effect on chlorophyll fluorescence (Ouyang et al. 2012). With the present microfluidic chip, the effects of $[\text{Cu}^{2+}]$ from

0 to 5 μM on the growth of *C. vulgaris* were investigated. Images of algae-encapsulated microdroplets with 0 and 5 μM of $[\text{Cu}^{2+}]$ at day 0 and day 10 are shown in Fig. 10a. *C. vulgaris* seemed to grow faster without the presence of $[\text{Cu}^{2+}]$. Figure 10b indicates the quantitative data. Overall, compared to concentrations of 0 and 0.625 μM , $[\text{Cu}^{2+}]$ higher than 2.5 μM inhibited algae growth. The number of cells per droplet decreased with an increase in $[\text{Cu}^{2+}]$. For example, these numbers changed from < 2 at day 0 to about 13.5, 14.7, 10.3, 9.1, and 8 at day 9.5 for $[\text{Cu}^{2+}]$ of 0, 0.625, 2.5, 4.375, and 5 μM , respectively. A similar trend was observed in fitted growth rates, being 0.229, 0.234, 0.201, 0.201, and 0.17 d^{-1} for $[\text{Cu}^{2+}]$ of 0, 0.625, 2.5, 4.375, and 5 μM , respectively. It was therefore suggested that $[\text{Cu}^{2+}]$ of low concentrations (less than 0.625 μM) didn't affect the growth of *C. vulgaris*, but the growth could be inhibited beyond a critical value (2.5 μM). Ouyang et al. studied the effects of $[\text{Cu}^{2+}]$ at different concentrations on *C. vulgaris* growth in BG-11 medium, and found that a 5 μM treatment significantly inhibited the growth (Ouyang et al. 2012). It was also reported that the growth rate per unit time of *C. vulgaris* decreased with an increase in $[\text{Cu}^{2+}]$ from 1 to 10 μM (Mehta 1999). Kebeish et al. conducted a detailed study on how Cu affects the growth, bioactive metabolites, antioxidant enzymes and photosynthesis-related gene transcription in *C. vulgaris* (Kebeish 2014). Higher concentrations of $[\text{Cu}^{2+}]$ (3 and 4.5 μM) showed a relative reduction in algal growth rate, and significant increases in carotenoids, intracellular proline contents, and activity of antioxidant enzymes were observed following copper exposure (Kebeish 2014). It is concluded that the growth of *C. vulgaris* could be inhibited as the concentration of copper increased beyond a certain value (typically between 2.5 and 5 μM).

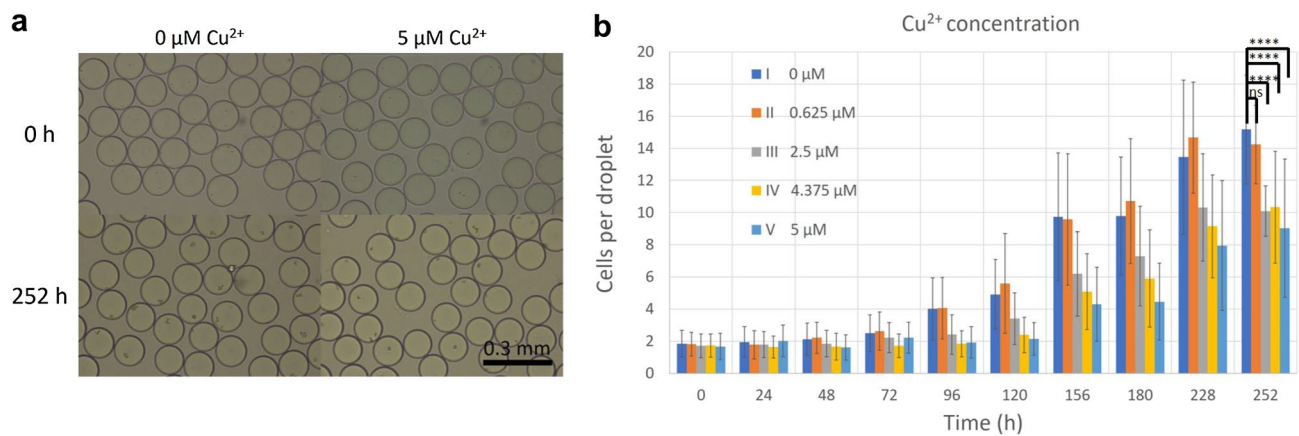


Fig. 10 **a** Images showing algae-encapsulated micro-droplets with 0 and 5 μM of Cu^{2+} in culture media at 0 h and 240 h **b** Quantitative data showing the growth of *C. vulgaris* when cultured in dif-

ferent [Cu^{2+}]. Statistical analysis was performed. ns: no statistically significant difference ($p > 0.05$); * $p < 0.05$; ** $p < 0.01$; *** $p < 0.001$; **** $p < 0.0001$

4 Conclusions

In this study, a microfluidic chip was successfully designed and fabricated for generating microalgae-encapsulated microdroplets. By modifying the "Christmas tree" structure, uniform flow rates in all outlets can be attained to synthesize droplets of consistent sizes, being around 125 μm in diameter and 1 nL in volume. Five sets of micro-droplets containing different media were generated simultaneously for culturing and investigating algae growth in a parallel and high-throughput manner. Microalgae *C. vulgaris* was incubated within these compartments and monitored for 10 days to track their numbers over time. The results indicated that the presence of nutrient and urea solutions at optimal concentrations stimulated the growth of *C. vulgaris*, but a highly nutrient medium or a concentrated urea solution could instead inhibit the growth. As for copper, low concentrations of Cu^{2+} (below 0.625 μM) didn't affect *C. vulgaris* growth much, but it could be suppressed as the concentration increased beyond a critical value (2.5 μM). These findings are of help to optimizing the growth of microalgae for increasing their potentials as resources of bio-products and biofuels. And this platform can be further applied to single cell-based investigations of more complicated animal and human cells in a high-throughput way.

Acknowledgements This work was financially supported by the Ministry of Science and Technology of Taiwan under Contract No. MOST 110-2112-M-030-002-MY2 and MOST 111-2112-M-030-004-. The authors also thank Prof. Si-Shen Li for help in providing microalgae and culture media.

Author contributions Y.-H.W. and Y.-S.S. designed the study and the microfluidic chip, carried out the experiments and data analysis, and interpreted the data. Y.-H.W. prepared all figures. Y.-S.S. drafted and reviewed the manuscript.

Data availability The data that support the findings of this study are available from the corresponding author upon reasonable request.

Declarations

Conflict of interest The authors have no relevant financial or non-financial interests to disclose.

References

- Ambati RR, Phang SM, Ravi S, Aswathanarayana RG (2014) Astaxanthin: sources, extraction, stability, biological activities and its commercial applications—a review. *Mar Drugs* 12:128–152. <https://doi.org/10.3390/md12010128>
- Beer LL, Boyd ES, Peters JW, Posewitz MC (2009) Engineering algae for biohydrogen and biofuel production. *Curr Opin Biotechnol* 20:264–271. <https://doi.org/10.1016/j.copbio.2009.06.002>
- Beneyton T, Thomas S, Griffiths AD, Nicaud JM, Drevelle A, Rosignol T (2017) Droplet-based microfluidic high-throughput screening of heterologous enzymes secreted by the yeast *Yarrowia lipolytica*. *Microb Cell Fact* 16:18. <https://doi.org/10.1186/s12934-017-0629-5>
- Best R, Abalde-Cela S, Abell C, Smith AG (2016) Applications of microdroplet technology for algal biotechnology. *Curr Biotechnol* 5:109–117
- Bialon J, Rath T (2018) Growth rates and photon efficiency of *Chlorella Vulgaris* in relation to photon absorption rates under different LED-types. *Algal Res* 31:204–215. <https://doi.org/10.1016/j.algal.2018.02.007>
- Brouzes E et al (2009) Droplet microfluidic technology for single-cell high-throughput screening. *Proc Natl Acad Sci USA* 106:14195–14200. <https://doi.org/10.1073/pnas.0903542106>
- Converti A, Scapazzoni S, Lodi A, Carvalho JCM (2006) Ammonium and urea removal by *Spirulina Platensis*. *J Ind Microbiol Biot* 33:8–16. <https://doi.org/10.1007/s10295-005-0025-8>
- Crofcheck C, Shea A, Montross M, Crocker M, Andrews R (2012) Influence of media composition on the growth rate of *Chlorella vulgaris* and *Scenedesmus acutus* utilized for CO₂ mitigation. *J Biochem Tech* 4:589–594

- Eastburn DJ, Sciambi A, Abate AR (2014) Identification and genetic analysis of cancer cells with PCR-activated cell sorting. *Nucleic Acids Res* 42:e128. <https://doi.org/10.1093/nar/gku606>
- El-Ali J, Sorger PK, Jensen KF (2006) Cells on chips. *Nature* 442:403–411
- Farjami T, Madadlou A (2017) Fabrication methods of biopolymeric microgels and microgel-based hydrogels. *Food Hydrocolloid* 62:262–272
- Fiebigler K, Gray T, Hood M, Hoepner J (2018) The effect of urea concentration in water on the growth of *Chlorella Algae*. *J Introd Biol Investig* 8:1–3
- Field CB, Behrenfeld MJ, Randerson JT, Falkowski P (1998) Primary production of the biosphere: integrating terrestrial and oceanic components. *Science* 281:237–240. <https://doi.org/10.1126/science.281.5374.237>
- Golterman HL, Clymo KE, Clymo RS (1975) Physiological limnology: an approach to the physiology of lake ecosystems. *Developments in water science*, vol 2. Elsevier, Amsterdam
- Gulati S, Vijayakumar K, Good WW, Tamayo WL, Patel AR, Niu XZ (2016) Microdroplet formation in rounded flow-focusing junctions. *Microfluid Nanofluid*. <https://doi.org/10.1007/s10404-015-1680-3>
- Hayat Z, El Abed AI (2018) High-throughput optofluidic acquisition of microdroplets in microfluidic systems. *Micromachines*. <https://doi.org/10.3390/mi9040183>
- Huang CH, Hou HS, Lo KY, Cheng JY, Sun YS (2017) Use microfluidic chips to study the effects of ultraviolet lights on human fibroblasts. *Microfluid Nanofluid*. <https://doi.org/10.1007/s10404-017-1922-7>
- Huang WM, Bi YH, Hu ZY (2014) Effects of fertilizer-urea on growth photosynthetic activity and microcystins production of microcystis aeruginosa isolated from Dianchi lake B. *Environ Contam Tox* 92:514–519. <https://doi.org/10.1007/s00128-014-1217-6>
- Jakiela S, Kaminski TS, Cybulski O, Weibel DB, Garstecki P (2013) Bacterial growth and adaptation in microdroplet chemostats. *Angew Chem* 52:8908–8911. <https://doi.org/10.1002/anie.201301524>
- Jang M, Yang S, Kim P (2016) Microdroplet-based cell culture models and their application. *Biochip J* 10:310–317
- Jeon NL, Dertinger SKW, Chiu DT, Choi IS, Stroock AD, Whitesides GM (2000) Generation of solution and surface gradients using microfluidic systems. *Langmuir* 16:8311–8316. <https://doi.org/10.1021/la000600b>
- Kaern M, Elston TC, Blake WJ, Collins JJ (2005) Stochasticity in gene expression: from theories to phenotypes nature reviews. *Genetics* 6:451–464. <https://doi.org/10.1038/nrg1615>
- Kebeish R, El-Ayouty Y, Husain A (2014) Effect of copper on growth, bioactive metabolites, antioxidant enzymes and photosynthesis-related gene transcription in *Chlorella vulgaris*. *World J Biol Sci* 2:034–043
- Khalili A, Najafpour GD, Amini G, Samkhaniani F (2015) Influence of nutrients and LED light intensities on biomass production of microalgae *Chlorella Vulgaris*. *Biotechnol Bioproc E* 20:284–290. <https://doi.org/10.1007/s12257-013-0845-8>
- Khan MI, Shin JH, Kim JD (2018) The promising future of microalgae: current status, challenges, and optimization of a sustainable and renewable industry for biofuels, feed, and other products. *Microbial Cell Fact* 17:36. <https://doi.org/10.1186/s12934-018-0879-x>
- Khemiri S, Bouchech I, Berrejeb N, Mejri M, Smaali I, Khelifi N (2022) Effects of growth medium variation on the nutri-functional properties of microalgae used for the enrichment of ricotta. *Food Technol Biotech* 60:29–40. <https://doi.org/10.17113/ftb.60.01.22.7105>
- Kim BI et al (2012) Synthesis of bioactive microcapsules using a microfluidic device. *Sensors* 12:10136–10147
- Lemoine Y, Schoefs B (2010) Secondary ketocarotenoid astaxanthin biosynthesis in algae: a multifunctional response to stress. *Photosynth Res* 106:155–177. <https://doi.org/10.1007/s11120-010-9583-3>
- Li J, Lin F (2011) Microfluidic devices for studying chemotaxis and electrotaxis. *Trends Cell Biol* 21:489–497. <https://doi.org/10.1016/j.tcb.2011.05.002>
- Liang F, Wen XB, Geng YH, Ouyang ZR, Luo LM, Li YG (2013) Growth Rate and Biomass Productivity of *Chlorella* as Affected by Culture Depth and Cell Density in an Open Circular Photobioreactor. *J Microbiol Biotechnol* 23:539–544. <https://doi.org/10.4014/jmb.1209.09047>
- Lin FY, Lin JY, Lo KY, Sun YS (2019) Use microfluidic chips to study the phototaxis of lung cancer cells. *Int J Molecular Sci*. <https://doi.org/10.3390/ijms20184515>
- Lo KY, Zhu Y, Tsai HF, Sun YS (2013) Effects of shear stresses and antioxidant concentrations on the production of reactive oxygen species in lung cancer cells. *Biomicrofluidics*. <https://doi.org/10.1063/1.4836675>
- Loizou K, Wong V-L, Hewakandamby B (2018) Examining the effect of flow rate ratio on droplet generation and regime transition in a microfluidic T-junction at constant capillary numbers. *Inventions* 3:1–17
- Mazutis L, Gilbert J, Ung WL, Weitz DA, Griffiths AD, Heyman JA (2013) Single-cell analysis and sorting using droplet-based microfluidics. *Nat Protoc* 8:870–891
- Mehta SKaG, J. P. (1999) Heavy-metal-induced proline accumulation and its role in ameliorating metal toxicity in *Chlorella vulgaris*. *New Phytol* 143:253–259
- Menetrez MY (2012) An overview of algae biofuel production and potential environmental impact. *Environ Sci Technol* 46:7073–7085. <https://doi.org/10.1021/es300917r>
- Mercer P, Armenta RE (2011) Developments in oil extraction from microalgae. *Eur J Lipid Sci Tech* 113:539–547
- Nan L, Jiang Z, Wei X (2014) Emerging microfluidic devices for cell lysis: a review. *Lab Chip* 14:1060–1073. <https://doi.org/10.1039/c3lc51133b>
- Nguyen TDP et al (2019) Investigation of the relationship between bacteria growth and lipid production cultivating of microalgae *Chlorella Vulgaris* in seafood. *Wastewater Energies*. <https://doi.org/10.3390/en12122282>
- Ouyang HL et al (2012) Effects of five heavy metals at sub-lethal concentrations on the growth and photosynthesis of *Chlorella Vulgaris*. *Chin Sci Bull* 57:3363–3370. <https://doi.org/10.1007/s11434-012-5366-x>
- Panis G, Carreon JR (2016) Commercial astaxanthin production derived by green alga *Haematococcus Pluvialis*: a microalgae process model and a techno-economic assessment all through production line. *Algal Res* 18:175–190
- Parmar A, Singh NK, Pandey A, Gnansounou E, Madamwar D (2011) Cyanobacteria and microalgae: a positive prospect for biofuels. *Biores Technol* 102:10163–10172. <https://doi.org/10.1016/j.biortech.2011.08.030>
- Radakovits R, Jinkerson RE, Darzins A, Posewitz MC (2010) Genetic engineering of algae for enhanced biofuel production. *Eukaryot Cell* 9:486–501. <https://doi.org/10.1128/EC.00364-09>
- Rahman NA, Katayama T, Wahid MEA, Kasan NA, Khatoun H, Yamada Y, Takahashi K (2020) Taxon- and growth phase-specific antioxidant production by chlorophyte, bacillariophyte, and haptophyte strains isolated from tropical waters front. *Bioeng Biotech*. <https://doi.org/10.3389/fbioe.2020.581628>
- Singh AK, Singh MP (2014) Importance of algae as a potential source of biofuel. *Cell Mol Biol (noisy-Le-Grand)* 60:106–109

- Stegeman GW, Medina D, Cutter AD, Ryu WS (2019) Neuro-genetic plasticity of *Caenorhabditis elegans* behavioral thermal tolerance. *BMC Neurosci* 20:26. <https://doi.org/10.1186/s12868-019-0510-z>
- Steinbrener J, Linden H (2001) Regulation of two carotenoid biosynthesis genes coding for phytoene synthase and carotenoid hydroxylase during stress-induced astaxanthin formation in the green alga *Haematococcus pluvialis*. *Plant Physiol* 125:810–817. <https://doi.org/10.1104/pp.125.2.810>
- Sun YS (2017) Studying electrotaxis in microfluidic devices. *Sensors*. <https://doi.org/10.3390/s17092048>
- Vo Hoang Nhat P et al (2018) Can algae-based technologies be an affordable green process for biofuel production and wastewater remediation? *Biores Technol* 256:491–501. <https://doi.org/10.1016/j.biortech.2018.02.031>
- Wojnicki M, Luty-Blocho M, Hessel V, Csapo E, Ungor D, Fitzner K (2018) Micro droplet formation towards continuous nanoparticles synthesis. *Micromachines* 9:248
- Wong YK, Ho YH, Ho KC, Leung HM, Yung KKL (2017) Growth medium screening for *Chlorella vulgaris* growth and lipid productions. *J Aquac Mar Biol* 6:1–7
- Wu L, Chen P, Dong YS, Feng XJ, Liu BF (2013) Encapsulation of single cells on a microfluidic device integrating droplet generation with fluorescence-activated droplet sorting. *Biomed Microdevices* 15:553–560
- Wu SY, Hou HS, Sun YS, Cheng JY, Lo KY (2015) Correlation between cell migration and reactive oxygen species under electric field stimulation. *Biomicrofluidics*. <https://doi.org/10.1063/1.4932662>
- Yun YS, Park JM (2003) Kinetic modeling of the light-dependent photosynthetic activity of the green microalga *Chlorella vulgaris*. *Biotechnol Bioeng* 83:303–311. <https://doi.org/10.1002/bit.10669>
- Zhu P, Wang L (2016) Passive and active droplet generation with microfluidics: a review. *Lab Chip* 17:34–75. <https://doi.org/10.1039/c6lc01018k>

Publisher's Note Springer Nature remains neutral with regard to jurisdictional claims in published maps and institutional affiliations.

Springer Nature or its licensor (e.g. a society or other partner) holds exclusive rights to this article under a publishing agreement with the author(s) or other rightsholder(s); author self-archiving of the accepted manuscript version of this article is solely governed by the terms of such publishing agreement and applicable law.